

# The piezoelectric and dielectric properties of PZT–PMN–PZN

C.H. Wang

*Department of Electronic Engineering, Nan-Jeon Institute of Technology, Tainan 737, Taiwan*

Received 22 July 2002; received in revised form 10 May 2003; accepted 10 July 2003

## Abstract

The dielectric and piezoelectric properties of  $\text{Pb}_{0.96}\text{Sr}_{0.04}[(\text{Zr}_{1-y}\text{Ti}_y)_{0.74}(\text{Mg}_{1/3}\text{Nb}_{2/3})_{0.20}(\text{Zn}_{1/3}\text{Nb}_{2/3})_{0.06}]\text{O}_3$  were investigated in the composition range  $0.47 \leq y \leq 0.57$ . The piezoelectric ceramic system of  $\text{PbTiO}_3$ – $\text{PbZrO}_3$ – $\text{Pb}(\text{Mg}_{1/3}\text{Nb}_{2/3})\text{O}_3$ – $\text{Pb}(\text{Zn}_{1/3}\text{Nb}_{2/3})\text{O}_3$  with composition close to the morphotropic phase boundary was studied. Results of XRD and piezoelectric measurement indicated that the  $y = 0.51$  composition corresponds to morphotropic phase boundary (MPB) between tetragonal and pseudocubic perovskite. Owing to the phase coexistence at the phase boundary, there exists a different symmetry regions (DSR) near the MPB. The DSR boundary motion increases the dielectric permittivity and piezoelectric coefficients. The planar coupling factor and piezoelectric constant are higher for compositions near the MPB, but longitudinal velocity are lowest. The reason for the decrease of the velocity at the phase boundary is considered as the existence of the DSR. Owing to the DSR comprising the tetragonal phase and the pseudocubic phase, the interphase boundaries make the extra scattering of the velocity comparing to other composition. As far as the dielectric constant of poled material is concerned, its maximum in the multicomponent system is displaced into the tetragonal phase and does not coincide with the maximum of planar coupling factor. The variation of the remanent polarization with composition is the same as that of the coupling factor.

© 2003 Elsevier Ltd and Techna Group S.r.l. All rights reserved.

**Keywords:** C. Dielectric properties; C. Piezoelectric properties; D. PZT; MPB; DSR

## 1. Introduction

Since Jaffe et al. [1] found that lead zirconate titanate  $\text{Pb}(\text{Ti,Zr})\text{O}_3$  had a high potential as an electromechanical transducer material, several tentative studies were carried out to improve the performance of these ceramics by doping with some minor additives or synthesizing the multicomponent solid solution with complex perovskite structure.

However, when two kinds of minor additives were added simultaneously, much improved piezoelectric properties could be obtained. Therefore, ternary solid-solution ceramics are being synthesized in place of the binary ceramics, consisting of a complex perovskite compound; (Zr,Ti) is substituted by  $(\text{Mg}_{1/3}\text{Nb}_{2/3})$  [2],  $(\text{Zn}_{1/3}\text{Nb}_{2/3})$  [3],  $(\text{Mn}_{1/3}\text{Nb}_{2/3})$  [4], and  $(\text{Co}_{1/3}\text{Nb}_{2/3})$  [5] to form ternary ceramic system and eventually a multicomponent system of complex oxide.

As for the multicomponent system synthesized by more than one complex oxide, it is more advantageous for adjusting its properties. Three quaternary ceramic system  $\text{Pb}$ –

$(\text{Mn}_{1/3}\text{Nb}_{2/3})\text{O}_3$ – $\text{Pb}(\text{Zn}_{1/3}\text{Nb}_{2/3})\text{O}_3$ – $\text{PbTiO}_3$ – $\text{PbZrO}_3$ ,  $\text{Pb}$ – $(\text{Mg}_{1/3}\text{Nb}_{2/3})\text{O}_3$ – $\text{Pb}(\text{Co}_{1/3}\text{Nb}_{2/3})\text{O}_3$ – $\text{PbTiO}_3$ – $\text{PbZrO}_3$  and  $\text{Pb}(\text{Ni}_{1/3}\text{Nb}_{2/3})\text{O}_3$ – $\text{Pb}(\text{Zn}_{1/3}\text{Nb}_{2/3})\text{O}_3$ – $\text{PbTiO}_3$ – $\text{PbZrO}_3$  are described by Wu et al. [6], Lee et al. [7] and Chung et al. [8], respectively. The former is a hard-type ceramic system with a high mechanical quality factor ( $Q_m = 960$ ) and lower planar coupling factor ( $k_p = 0.47$ ) at the phase boundary. In the  $\text{Pb}(\text{Mg}_{1/3}\text{Nb}_{2/3})\text{O}_3$ – $\text{Pb}(\text{Co}_{1/3}\text{Nb}_{2/3})\text{O}_3$ – $\text{PbTiO}_3$ – $\text{PbZrO}_3$  system, it is a soft-type ceramic system with good planar coupling factor and nearly zero aging rate of resonant frequency. The last is also a soft-type ceramic system with a high dielectric constant 6200 and piezoelectric strain constant  $0.38 \times 10^{-9} \text{ C N}^{-1}$ .

In the present work,  $\text{Pb}(\text{Mg}_{1/3}\text{Nb}_{2/3})\text{O}_3$ – $\text{Pb}(\text{Zn}_{1/3}\text{Nb}_{2/3})\text{O}_3$ – $\text{PbTiO}_3$ – $\text{PbZrO}_3$  with compositions close to morphotropic phase boundary (MPB) were studied for high sensitive applications. Here, because partial substitution of Sr for Pb can not only increase dielectric constant, but also to be effective as a fluxing agent [9]. Therefore, the dielectric and piezoelectric properties of  $\text{Pb}_{0.96}\text{Sr}_{0.04}[(\text{Zr}_{1-y}\text{Ti}_y)_{0.74}(\text{Mg}_{1/3}\text{Nb}_{2/3})_{0.20}(\text{Zn}_{1/3}\text{Nb}_{2/3})_{0.06}]\text{O}_3$  ceramics were obtained by changing the content of main compounds,  $\text{TiO}_2$ .

E-mail address: [wch70982@ms41.hinet.net](mailto:wch70982@ms41.hinet.net) (C.H. Wang).

## 2. Experimental procedure and measurement

The compositions used in this study were  $\text{Pb}_{0.96}\text{Sr}_{0.04}[(\text{Zr}_{1-y}\text{Ti}_y)_{0.74}(\text{Mg}_{1/3}\text{Nb}_{2/3})_{0.20}(\text{Zn}_{1/3}\text{Nb}_{2/3})_{0.06}]\text{O}_3$  with  $0.47 \leq y \leq 0.57$ . All the specimens were prepared by conventional ceramic technology. Raw materials were mixed from pure reagent-grade (>99%)  $\text{PbO}$ ,  $\text{SrCO}_3$ ,  $\text{ZrO}_2$ ,  $\text{TiO}_2$ ,  $\text{MgO}$ ,  $\text{Nb}_2\text{O}_5$  and  $\text{ZnO}$ . Excess 0.5 wt.%  $\text{PbO}$  was added to the solid solution to enhance the formation of a liquid phase, which served as a densification promoter [10]. A mixture of the starting powders homogenized with acetone was mixed and milled in an alumina ball mill for 4 h. After that, the mixture was dried and calcined at  $920^\circ\text{C}$  for 2 h in an alumina crucible. The reacted material was ground and then pressed into a disc shape under  $700\text{ kg cm}^{-2}$ . The size of the green compact was 14 mm in diameter and 1 mm in thickness. The samples were covered with an alumina crucible and sintered at  $1250^\circ\text{C}$  for 3 h. To provide a positive vapor pressure,  $\text{PbZrO}_3$  with 3 wt.% excess  $\text{PbO}$  was used as the packing powder. After sintering, the lapped and polished samples were printed with silver paste on each surface and fired at  $700^\circ\text{C}$  ready for the poling process. The poling technique was generally to immerse the samples into silicone oil suffering from dielectric breakdown, and poled by  $3\text{ kV cm}^{-1}$  at  $100^\circ\text{C}$  for 30 min.

In order to determine crystal structure and crystal system, the sintered ceramic samples were polished, and measurements carried out at room temperature by the X-ray diffraction (XRD) method using  $\text{Cu K}\alpha$  radiation. By means of a scanning electron microscope (SEM), the free surface of the sintered ceramic body was observed. The mean grain size was calculated by the line intercept method [11]. The density was measured by water displacement method. The  $P$ – $E$  hysteresis loop was observed with a modified Sawyer–Tower circuit. Finally, dielectric and piezoelectric properties were measured with an HP4192A LF Impedance Analyser with reference of the IRE Standards [12]. By using the Parametric Model 5218 Ultrasonic Thickness Gage, the longitudinal wave velocity was measured in both poled and unpoled piezoelectric discs. The piezoelectric strain constant  $d_{33}$  was measured by  $d_{33}$  meter.

## 3. Results and discussion

### 3.1. X-ray diffraction

XRD patterns of the  $\text{Pb}_{0.96}\text{Sr}_{0.04}[(\text{Zr}_{1-y}\text{Ti}_y)_{0.74}(\text{Mg}_{1/3}\text{Nb}_{2/3})_{0.20}(\text{Zn}_{1/3}\text{Nb}_{2/3})_{0.06}]\text{O}_3$  system with different compositions ( $y = 0.47$ ,  $y = 0.51$ ,  $y = 0.52$  and  $y = 0.57$ ) at room temperature are shown in Fig. 1. The X-ray peak (200) at  $44.5^\circ$  of Fig. 1b split apparently up into two peaks (002 and 200) at  $44^\circ$  and  $45^\circ$  of Fig. 1c, respectively. Perovskite phase appears to have pseudocubic symmetry for  $y$  less than 0.51 and tetragonal symmetry for  $y$  greater than

0.51. A morphotropic transformation between pseudocubic and tetragonal phases was found at  $y$  close to 0.51.

### 3.2. Hysteresis loop

The hysteresis loop is one of the most important characteristics of a ferroelectric and gives information on its dynamic polarizability. The  $P$ – $E$  curves of the system are shown in Fig. 2a–c. Fig. 3 shows the remnant polarization ( $P_r$ ) and coercive field ( $E_c$ ) as a function of the composition. The remnant polarization ( $P_r$ ) also increases until it reaches a peak value at the phase boundary, then decreases for higher Ti concentration. The  $P_r$  has a maximum value at the phase boundary. It may be the reason that the phase coexistence offers more polarization at the phase boundary [13–16]. On the other hand, Benguigui [17] used Landau–Devonshire theory [18] to explain the phenomena. The tetragonal phase obviously have a higher  $E_c$  than the pseudocubic phase in Fig. 3. The coercive field is nearly constant for the pseudocubic composition, but it increases with increasing  $\text{PbTiO}_3$  in the tetragonal region. Thus, compositions with the tetragonal phase are “ferroelectrically harder” and those with the pseudocubic phase “ferroelectrically softer” than composition close to the morphotropic phase boundary.

### 3.3. Density

It is difficult to obtain a well sintered body of  $\text{PbTiO}_3$  and  $\text{PbZrO}_3$ , because  $\text{PbTiO}_3$  has an abnormally anisotropic crystallographic transformation at the curie temperature of  $490^\circ\text{C}$  and  $\text{PbZrO}_3$  shows violent evaporation of  $\text{PbO}$ . However, the  $\text{PbTiO}_3$ – $\text{PbZrO}_3$ – $\text{Pb}(\text{Mg}_{1/3}\text{Nb}_{2/3})$ – $\text{Pb}(\text{Zn}_{1/3}\text{Nb}_{2/3})\text{O}_3$  compositions are free from these difficulties and sintering becomes much easier. All of the compositions are sintered in an air environment with providing positive Pb atmosphere control at  $1250^\circ\text{C}$  for 3 h. The real density of the sintered samples is 90–96% of the theoretical density. In general, the real density increases with an increase of  $\text{PbTiO}_3$  until it reaches a peak value at the phase boundary, then decreases for higher concentrations as in shown Fig. 4. The results agree with that observed by Tawfik et al. [19]. It may be explained by the sintering model of Coble [20] that the existence of the DSR will offer the interphase boundary as a sink of defect or vacancy resulting in the increase of the density.

### 3.4. Electromechanical coupling factor

The electromechanical coupling factor is related to different  $\text{PbTiO}_3$  concentration as shown in Fig. 5. The planar coupling factor ( $k_p$ ) has been used extensively as a measure of the piezoelectric response of PZT type ceramics. It was found that  $k_p$  depended on the material parameters [21] such as grain size, porosity, and chemical composition. Piezoelectric activity reaches a maximum, when ceramic

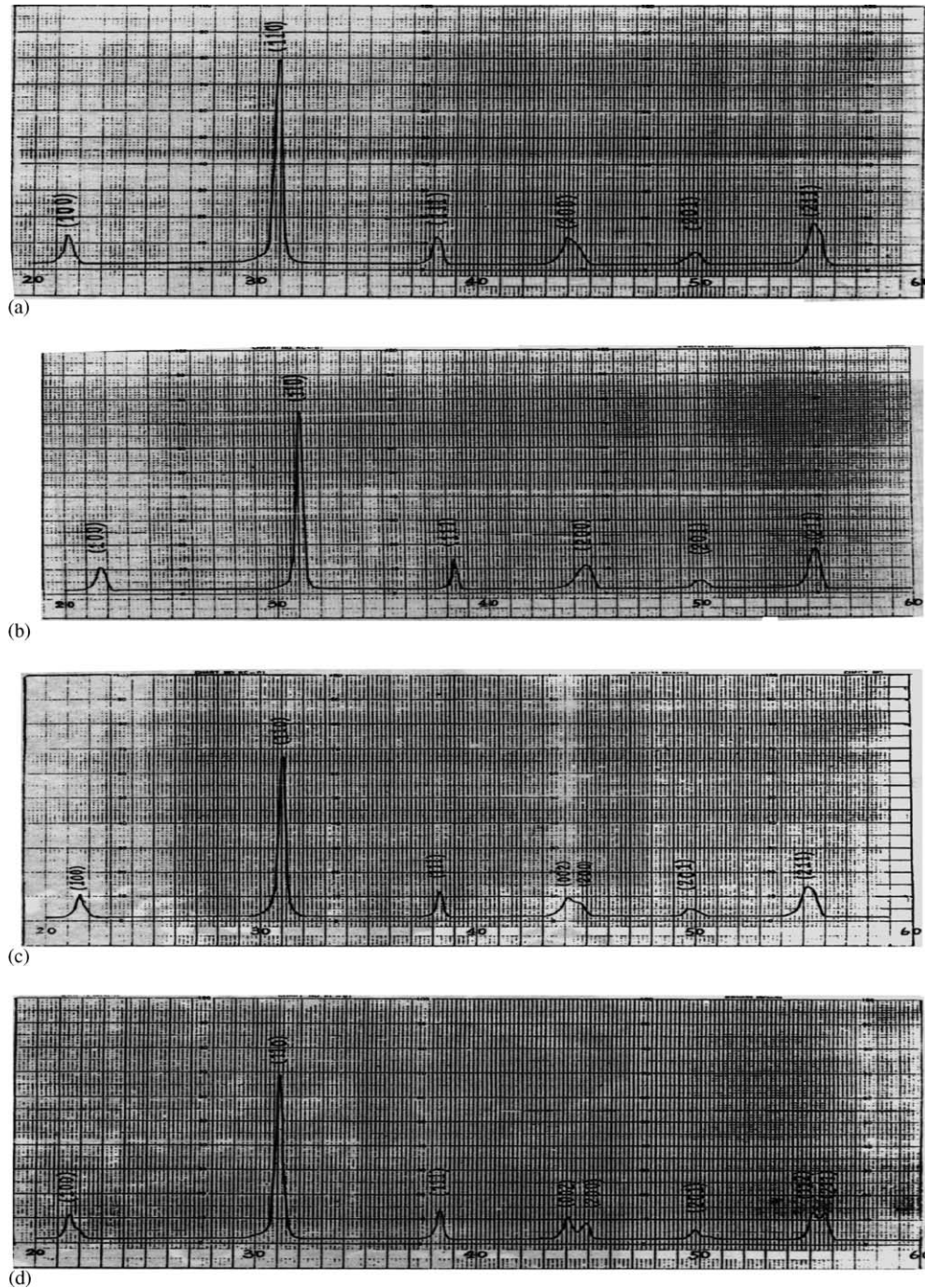


Fig. 1. XRD patterns of the  $\text{Pb}_{0.96}\text{Sr}_{0.04}[(\text{Zr}_{1-y}\text{Ti}_y)_{0.74}(\text{Mg}_{1/3}\text{Nb}_{2/3})_{0.20}(\text{Zn}_{1/3}\text{Nb}_{2/3})_{0.06}]\text{O}_3$  samples with different compositions: (a)  $y = 0.47$ , (b)  $y = 0.51$ , (c)  $y = 0.52$  and (d)  $y = 0.57$  at room temperature.

compositions are chosen near those of the morphotropic phase boundary. Usually, the piezoelectric activity is appreciated by the value of the electromechanically coupling factor in radial mode  $k_p$ . Therefore,  $k_p$  is the figure of merit of the piezoelectric activity and the square of that gives the efficiency of the conversion of electrical-mechanical energy [22]. The highest coupling factor is found at the phase boundary.

### 3.5. Dielectric constant

In piezoelectric ceramics, the properties depend on the composition and crystal structure; the dielectric constant may be increased or decreased through poling treatment. Fig. 6 shows the dielectric constant  $K$  (before polarization) and  $K_{33}^T$  (after polarization) of the system. After poling, the dielectric constant increases for the tetragonal compositions,



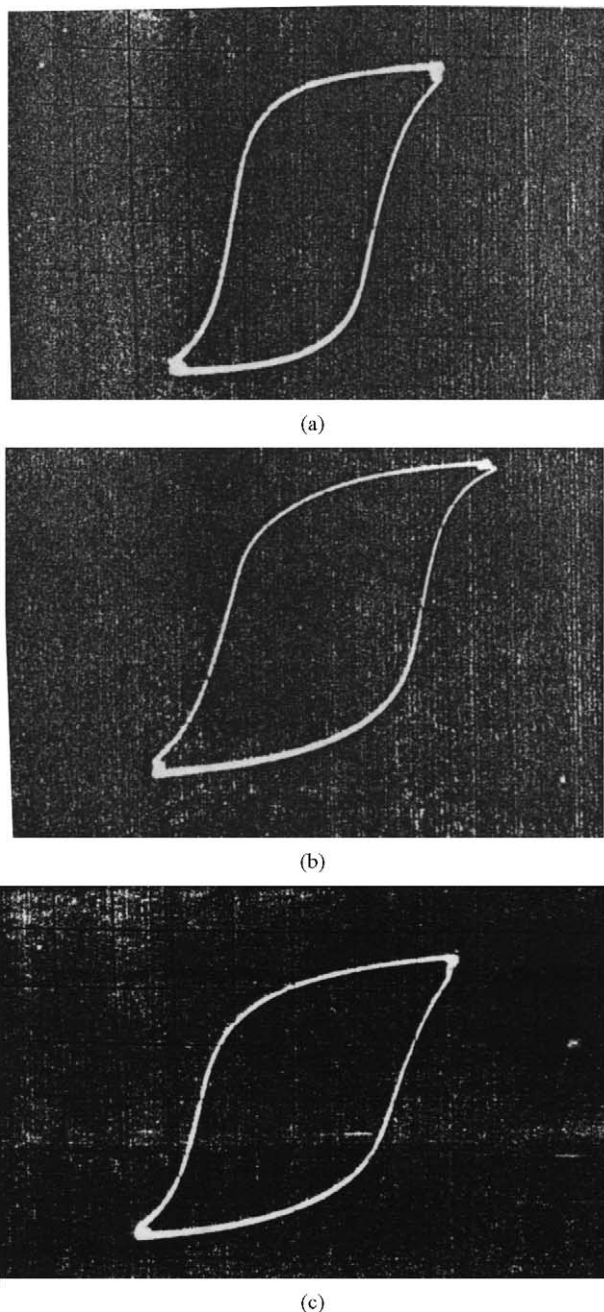


Fig. 2. Variation of the  $P$ - $E$  hysteresis loop of  $\text{Pb}_{0.96}\text{Sr}_{0.04}[(\text{Zr}_{1-y}\text{Ti}_y)_{0.74}(\text{Mg}_{1/3}\text{Nb}_{2/3})_{0.20}(\text{Zn}_{1/3}\text{Nb}_{2/3})_{0.06}]\text{O}_3$  system with different compositions: (a)  $y = 0.50$ , (b)  $y = 0.51$ , (c) and  $y = 0.52$  at room temperature.

but decreases for the pseudocubic compositions. Moreover, the variations of the dielectric constant through poling also rely on the domain alignment. The increase of the dielectric constant of the poled tetragonal compositions is previously explained [23] as being due to the elimination of the effect of compression of the  $180^\circ$  domains. This occurs due to the virtually complete  $180^\circ$  domain reorientation along the poling direction, and dominates the decrease in dielectric constant from the  $90^\circ$  domain reorientation. In a pseudocubic

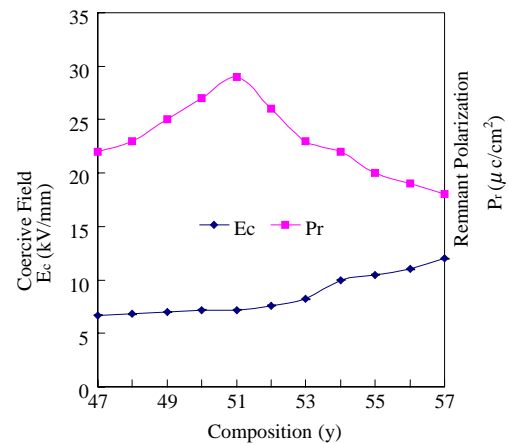


Fig. 3. Variation of the remnant polarization ( $P_r$ ) and the coercive field ( $E_c$ ) of  $\text{Pb}_{0.96}\text{Sr}_{0.04}[(\text{Zr}_{1-y}\text{Ti}_y)_{0.74}(\text{Mg}_{1/3}\text{Nb}_{2/3})_{0.20}(\text{Zn}_{1/3}\text{Nb}_{2/3})_{0.06}]\text{O}_3$  system as a function of the composition.

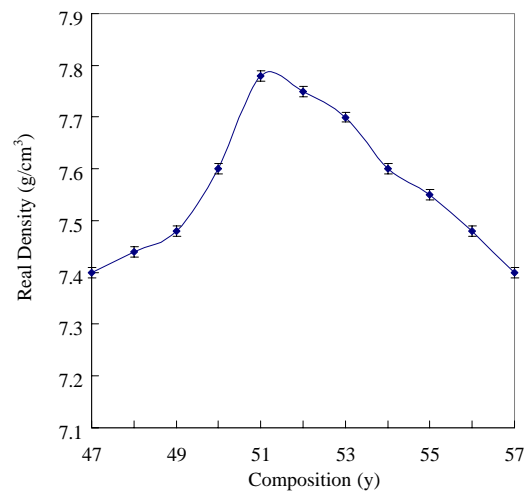


Fig. 4. Variation of the real density of  $\text{Pb}_{0.96}\text{Sr}_{0.04}[(\text{Zr}_{1-y}\text{Ti}_y)_{0.74}(\text{Mg}_{1/3}\text{Nb}_{2/3})_{0.20}(\text{Zn}_{1/3}\text{Nb}_{2/3})_{0.06}]\text{O}_3$  system as a function of the composition.

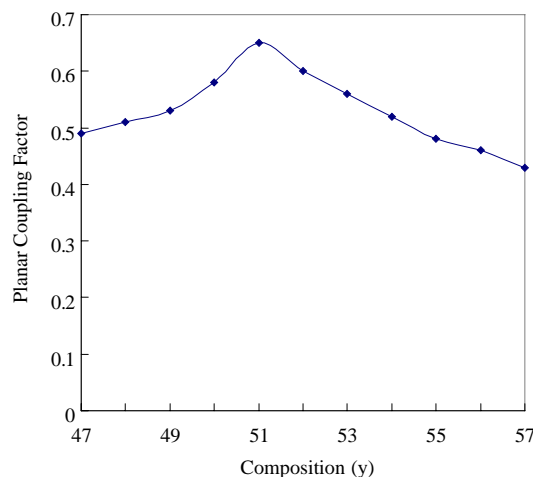


Fig. 5. Variation of the electromechanical coupling factor ( $k_p$ ) of  $\text{Pb}_{0.96}\text{Sr}_{0.04}[(\text{Zr}_{1-y}\text{Ti}_y)_{0.74}(\text{Mg}_{1/3}\text{Nb}_{2/3})_{0.20}(\text{Zn}_{1/3}\text{Nb}_{2/3})_{0.06}]\text{O}_3$  system as a function of the composition.

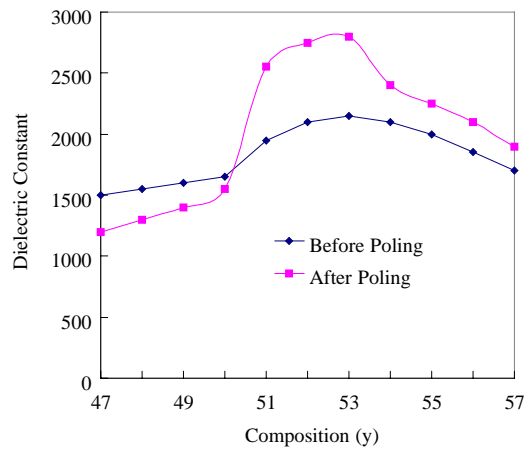


Fig. 6. Variation of the dielectric constant  $K$  (before polarization) and  $K_{33}^T$  (after polarization) of  $\text{Pb}_{0.96}\text{Sr}_{0.04}[(\text{Zr}_{1-y}\text{Ti}_y)_{0.74}(\text{Mg}_{1/3}\text{Nb}_{2/3})_{0.20}(\text{Zn}_{1/3}\text{Nb}_{2/3})_{0.06}]\text{O}_3$  system as a function of the composition.

phase, the dielectric constant decreases after poling, and the net decrease is owing to the  $90^\circ$  domain reorientation dominating the effect of the removal of compression [24,25]. In the pseudocubic region,  $K_{33}^T$  is decreasing in comparison to  $K$  as a result of the dielectric anisotropic; and in the tetragonal region,  $K_{33}^T$  is increasing because of relieving the clamping effect. This leads to a rise of dielectric constant in the tetragonal branch and to a decrease in the pseudocubic branch.

As far as dielectric constant of polarized ceramic is concerned, its maximum in multicomponent systems is displaced into tetragonal phase and does not coincide with the maximum of electromechanical coupling factor. The reasons of displacement of maximum  $K_{33}^T$  into tetragonal phase can be explained by Fesenko et al. [24].

### 3.6. Longitudinal wave velocity

Fig. 7 shows the longitude wave velocity ( $v$ ) has a minimum value at the phase boundary and the wave velocity is faster after poling. Before polarization the directions of the domains were very random and the domain walls make the scattering of the sound wave. After polarization, most directions of the domains are forced along the polarization and the scattering of the sound wave is reduced, leading to the increase of the  $v$  [26]. The reason for the decrease of  $v$  at the phase boundary is considered as the existence of the DSR. The DSR means the regions of the tetragonal phase are in the pseudocubic grains and the regions of the pseudocubic phase are in tetragonal grains. Owing to the DSR comprising the tetragonal phase and the pseudocubic phase, the interphase boundaries make the extra scattering of the  $v$  comparing to other composition.

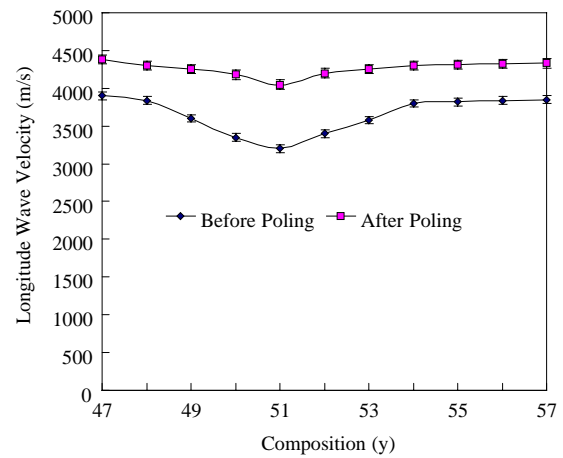


Fig. 7. Variation of the longitude wave velocity ( $v$ ) of  $\text{Pb}_{0.96}\text{Sr}_{0.04}[(\text{Zr}_{1-y}\text{Ti}_y)_{0.74}(\text{Mg}_{1/3}\text{Nb}_{2/3})_{0.20}(\text{Zn}_{1/3}\text{Nb}_{2/3})_{0.06}]\text{O}_3$  system as a function of the composition.

### 3.7. Frequency constant

The frequency constant ( $N_p$ ) were obtained by following equation:  $N_p = f_r \times D$  (Hz m), where  $D$  is the electrode diameter of the sample,  $f_r$  is the resonant frequency. If the  $D$  was fixed, then  $N_p$  was proportion to  $f_r$ . According to Fig. 8, in the solid solution near the MPB a steep decrease in  $N_p$  continues with a quite large fall in  $N_p$  being achieved at the minimum. Isupov [15,16] used the DSR to explain the phenomena. According to Isupov's result, it can be inferred that owing to the interphase boundary of the DSR limits the movement of the domains leading to the decrease of the  $f_r$ .

Here piezoelectric parameters corresponding to vibration modes involved will be calculated according to IRE standard on piezoelectric crystals to meet this demand [11]. The

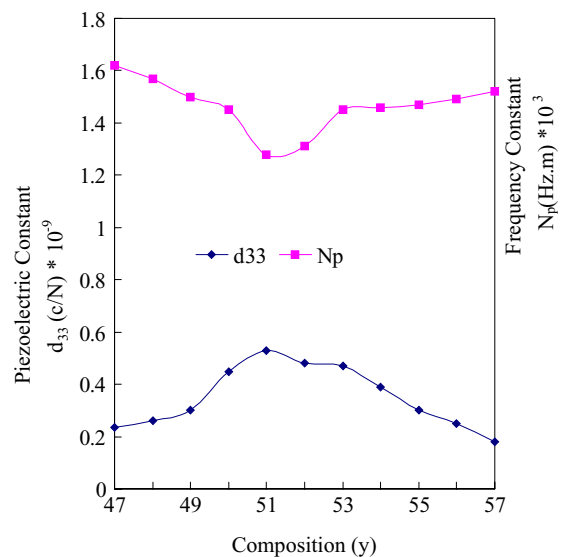


Fig. 8. Variation of the frequency constant ( $N_p$ ) and piezoelectric strain constant ( $d_{33}$ ) of  $\text{Pb}_{0.96}\text{Sr}_{0.04}[(\text{Zr}_{1-y}\text{Ti}_y)_{0.74}(\text{Mg}_{1/3}\text{Nb}_{2/3})_{0.20}(\text{Zn}_{1/3}\text{Nb}_{2/3})_{0.06}]\text{O}_3$  system as a function of the composition.

variation of piezoelectric constant ( $d_{33}$ ) as a function of Ti composition is shown in Fig. 8. It is found the piezoelectric constant is higher near the MPB region. The maximum value is  $0.533 \times 10^{-9} \text{ C N}^{-1}$  at  $y = 0.51$ .

#### 4. Conclusions

In the four component system PZ–PT–PMN–PZN with constant amount of PMN (20 mol%) and PZN (6 mol%), the MPB exists at which the amount of PT is nearly equal to 37.74 mol%. There are two phases in this system. When the amount of PT is less than 37.74 mol%, the structure is perovskite phase with pseudocubic symmetry, but after that is tetragonal symmetry.

In piezoelectric ceramics, depending on the crystalline phase, the dielectric constant may increase or decrease through poling treatment. In this system, the dielectric constant before polization is larger than that after polarization in pseudocubic region, but in the tetragonal region, the dielectric constant inversely. As far as the dielectric constant of poled ceramic is concerned, its maximum in the multi-component system is displaced into the tetragonal phase and does not coincide with the maximum of electromechanical coupling factor. Before and after poling, compositions close to the MPB are characterized by the smallest velocity of the longitudinal sound wave. Further, the longitudinal wave velocity of poled samples is higher than that of unpoled ones.

Owing to the phase coexistence at the phase boundary, there exists a DSR near the MPB. The DSR boundary motion increases the dielectric permittivity and piezoelectric coefficients. Owing to the DSR comprising the tetragonal phase and the pseudocubic phase, the interphase boundaries make the extra scattering of the longitudinal wave velocity comparing to other composition. This is the main reason, the existence of the DSR, for the decrease of  $v$  at the phase boundary. The DSR also can explain the lowest value of the frequency constant at the phase boundary. The interphase boundary of the DSR limits the movement of the domains leading to the decrease of the frequency constant  $f_r$ .

The hysteresis loop gives information on the dynamic polarizability. The coercive field ( $E_c$ ) is nearly constant for pseudocubic compositions but it will increase with increasing  $\text{PbTiO}_3$  in the tetragonal region. The variation of remanent polarization with composition is the same as that of the coupling factor. Thus, compositions with the tetragonal phase are “ferroelectrically harder” and those with the pseudocubic phase are “ferroelectrically softer” than compositions close to the MPB.

The PZT–PMN–PZN system in the vicinity of the MPB has an excellent dielectric and piezoelectric properties for wide practical application. The planar coupling factor (0.65), poled dielectric constant (2600), longitude wave velocity ( $4100 \text{ m s}^{-1}$ ), frequency constant (1280 Hz m) and  $d_{33}$  ( $533 \times 10^{-12} \text{ C N}^{-1}$ ) are attained in this system.

#### Acknowledgements

The author would like to acknowledge the financial support of the Nation Science Council (under contract NSC-90-2215-E-232-002) of the Republic of China.

#### References

- [1] B. Jaffe, W.R. Cook, H. Jaffe, *Piezoelectric Ceramics*, Academic Press, New York, 1971, p. 259.
- [2] K. Uchino, S. Nomura, L.E. Cross, S.J. Jang, R.E. Newnham, Electrostrictive effect in lead magnesium niobate single crystals, *J. Appl. Phys.* 51 (2) (1980) 1142–1145.
- [3] S. Choi, Y. Kim, H. Weon, Y. Shin, Dielectric, piezoelectric and pyroelectric properties in the  $(1-x) \text{Pb}(\text{Mg}_{0.7}\text{Zn}_{0.3})_{1/3}\text{Nb}_{2/3}\text{O}_3$ – $x\text{PbTiO}_3$  system, *Ferroelectrics* 158 (1994) 247–252.
- [4] K. Frank, Electromechanical properties of lead titanate zirconate ceramics modified with certain three- or five-valent additions, *J. Am. Ceram. Soc.* 42 (1) (1959) 343–349.
- [5] T. Kudo, Characteristics and dielectric properties of  $\text{PbTiO}_3$ – $\text{PbZrO}_3$ – $\text{Pb}(\text{Co}_{1/3}\text{Nb}_{2/3})\text{O}_3$  ceramics, *J. Am. Ceram. Soc.* 53 (6) (1970) 326–328.
- [6] L. Wu, C.H. Liang, C.F. Shieu, Piezoelectric properties of  $(\text{Pb}, \text{Sr})(\text{Zr}, \text{Ti}, \text{Mn}, \text{Zn}, \text{Nb})\text{O}_3$  piezoelectric ceramics, *J. Mater. Sci.* 26 (1991) 4439–4444.
- [7] M.H. Lee, K.H. Kim, C.K. Yang, Piezoelectric and dielectric properties of  $\text{Pb}(\text{Mg}, \text{Nb})\text{O}_3$ – $\text{Pb}(\text{Co}, \text{Nb})\text{O}_3$ – $\text{PbTiO}_3$ – $\text{PbZrO}_3$  system ceramics, in: *Proceedings of the IEEE Ultrasonic Symposium*, 1986, pp. 422–428.
- [8] S.T. Chung, K. Nagata, H. Igarashi, Piezoelectric and dielectric properties of  $\text{PbTiO}_3$ – $\text{PbZrO}_3$ – $\text{Pb}(\text{Ni}, \text{Nb})\text{O}_3$ – $\text{Pb}(\text{Zn}, \text{Nb})\text{O}_3$  system ceramics, *Ferroelectrics* 94 (1989) 243–247.
- [9] K. Frank, Electromechanical properties of lead titanate zirconate ceramics with lead partially replaced by calcium or strontium, *J. Am. Ceram. Soc.* 42 (1) (1959) 49–51.
- [10] J.P. Guha, U. Anderson, D.J. Hong, Effect of excess  $\text{PbO}$  on the sintering characteristics and dielectric properties of  $\text{PbTiO}_3$ – $\text{Pb}(\text{Mg}_{1/3}\text{Nb}_{2/3})\text{O}_3$ -based ceramic, *J. Am. Ceram. Soc.* 71 (3) (1988) C-152–C-154.
- [11] T. Senda, R.C. Bradt, Grain growth in sintered  $\text{ZnO}$  and  $\text{ZnO}$ – $\text{Bi}_2\text{O}_3$  ceramics, *J. Am. Ceram. Soc.* 73 (1) (1990) 106–114.
- [12] Anonymous, IRE standards on piezoelectric crystals: measurement of piezoelectric ceramics, *Proc. IRE.* 49 (1961) 1161–1168.
- [13] K. Kakegawa, J. Mohri, A compositional fluctuation and properties of  $\text{Pb}(\text{Zr}, \text{Ti})\text{O}_3$ , *Solid State Commun.* 24 (1977) 769–772.
- [14] K. Carl, K.H. Hardtl, Composition dependences in solid solutions on the basis of lead–zirconate–titanate and sodium niobate, *Phys. Status Solidi [a]* 8 (1971) 87–91.
- [15] V.A. Isupov, For discrepancies relating to the range of coexistence of phases in lead zirconate–titanate solid solutions, *Sov. Phys. Solid State* 12 (1970) 1084.
- [16] V.A. Isupov, The range of coexistence of phases in lead zirconate–titanate solid solutions, *Sov. Phys. Solid State* 10 (1968) 989.
- [17] L. Benguigui, Thermodynamic theory of the morphotropic phase transition tetragonal–rhombohedral in the perovskite ferroelectrics, *Solid State Commun.* 11 (1972) 825–828.
- [18] F. Devonshire, Thermodynamic theory of the morphotropic phase transition tetragonal–rhombohedral in lead zirconate–titanate solid solutions, *Phil. Mag.* 40 (1949) 1040.
- [19] A. Tawfik, F. ABD El. Salam, A.I. Eatah, Effect of zirconium concentration and doping with Sr and Al on the sintering and electromechanical properties of lead zirconate titanate ceramics, *Ferroelectrics* 65 (1985) 131–141.

- [20] R.L. Coble, Grain growth in sintered ZnO and ZnO–Bi<sub>2</sub>O<sub>3</sub> ceramics, *J. Appl. Phys.* 56 (1985) 131–141.
- [21] K. Okazaki, K. Nagata, Effects of grain size and porosity on electrical and optical properties of PLZT ceramics, *J. Am. Ceram. Soc.* 56 (2) (1973) 82–86.
- [22] K.H. Hartal, Physics of ferroelectric ceramics used in electronic devices, *Ferroelectrics* 12 (1976) 9–19.
- [23] V.A. Isupov, Yu.E. Stolypin, Coexistence of phases in lead zirconate–titanate solid solutions, *Sov. Phys. Solid State* 12 (1970) 2067–2071.
- [24] E.G. Fesenko, A.Y. Dantsiger, L.A. Resnitohenko, M.F. Kupriyanov, Composition–structure–properties dependences in solid solutions on the basis of lead–zirconate–titanate and sodium niobate, *Ferroelectrics* 41 (1982) 137–141.
- [25] V.A. Bokov, Dielectric properties of PbTiO<sub>3</sub>–PbZrO<sub>3</sub> ceramics, *Sov. Phys. Technol. Phys.* 2 (1957) 1657–1662.
- [26] P.S. Nicholson, N.D. Patel, Comparison of piezoelectric properties of hot-pressed and sintered PZT, *Am. Ceram. Soc. Bull.* 65 (1986) 783–787.